# Expression and Functional Involvement of Organic Anion Transporting Polypeptide Subtype 3 (*Slc21a7*) in Rat Choroid Plexus

**Hiroyuki Kusuhara,[1] Zhonggui He,[1] Yoshinori Nagata,[1] Yoshitane Nozaki,[1] Takashi Ito,[2] Hiroyuki Masuda,[2] Peter J. Meier,[3] Takaaki Abe,[4] and Yuichi Sugiyama[1,5]**

*Received October 15, 2002; accepted January 28, 2003*

***Purpose.*** It has been shown that transport(s) are involved in the uptake of estradiol 17β glucuronide (E217βG) by the choroid plexus (CP). The purpose of this study is to compare the substrate specificity of the transporter in the CP with those of rat organic anion transporting polypeptide 1 (rOatp1) and rOatp3.

***Methods.*** The expression of rOatp1 and rOatp3 in rat CP was confirmed by RT-PCR and Western blot analyses. The substrate specificity of rOatp1 and rOatp3 was compared using cDNA-transfected LLC-PK1 cells. The uptake of E217βG by rat isolated CP was determined by centrifugal filtration technique.

***Results.*** PCR analyses demonstrated that the mRNA expression of rOatp3 was abundant in the CP, whereas that of rOatp1 was low. Immunohistochemical staining revealed that rOatp3 is expressed on the apical membrane of the CP. Kinetic parameters ($K_m$ and $K_i$ values) of rOatp3 were similar to those for rOatp1. The results of mutual inhibition study suggest that E217βG and taurocholate share the same mechanism in the CP. Corticosterone, estrone-3-sulfate and indomethacin are moderate inhibitors, but no effects by digoxin, *p*-aminohippurate, benzylpenicillin and cimetidine were observed.

***Conclusions.*** rOatp3 is most possible candidate transporter involved in the uptake of organic anions on the brush border membrane of the choroid epithelial cells.

**KEY WORDS:** choroid plexus; blood-CSF barrier; efflux transport; Oatp; organic anion.

## INTRODUCTION

The choroid plexus (CP), located in the lateral, third and fourth ventricles, acts as a barrier between the cerebrospinal fluid (CSF) and the circulating blood and, thus, CP is referred to as the blood-CSF barrier (1–7). This barrier function is achieved partly by the tight monolayer of the choroid epithelial cells and partly by detoxification systems, such as metabolic enzymes and efflux transport systems at the CP (1–8).

Estradiol 17β glucuronide (E217βG) was rapidly removed from the CSF after intracerebroventricular administration (9). This was achieved by the efficient uptake system(s) for amphipathic organic anions located on the brush border membrane of the choroid epithelial cells (9–13). The uptake from the CSF is the initial process in overall elimination of organic substrates from the CSF. Organic anion transporting polypeptide 1 (rOatp1; Gene symbol *Slc21a1*) has been identified along the brush border membrane of choroid epithelial cells by anti-Oatp1 polyclonal antibody (12). rOatp1 has been shown to accept a variety of amphipathic organic anions such as bromosulfophthalein, bile acids, steroid conjugates such as E217βG and estrone sulfate and anionic drugs, including temocaprilat, enalapril and enalaprilat (ACE inhibitors), pravastatin (HMG-CoA reductase inhibitor), and CRC-220 (thrombin inhibitor) (14–20). Our preliminary RT-PCR analysis, however, revealed the expression of rOatp3 (*Slc21a7*) in the choroid plexus. rOatp3 is an isoform of rOatp1 and exhibits 80% identity with rOatp1 at the amino acid level (21). Its tissue distribution remains controversial. Northern blot analysis indicates its expression in the kidney when a fragment from the 3′ untranslational region of Oatp3 was used as probe (21). On the other hand, RNase protection assays indicated that rOatp3 is expressed in brain and small intestine but not in liver and kidney (22). Recently, Li *et al.* quantified mRNA expression of rOatp3 in ten tissues, and found most abundant expression in lung, moderate expression in cerebellum and female cortex, and low expression in other tissues, including small intestine (23). The substrates of rOatp3, include taurocholate (TCA), bromosulfophthalein, steroid conjugates, such as E217βG and estrone-3-sulfate, and thyroid hormones (20,21). The substrate specificity of rOatp3 is also similar to those of other Oatps although the affinities for some substrates are lower, and prostagladin E2 has been reported to be selectively transported by rOatp3 but not by rOatp1 or rOatp2 (20). The purpose of this study is to investigate the uptake mechanism of amphipathic organic anions in the CP, and possible role of rOatp3 in the CP.

## MATERIALS AND METHODS

### Materials

[$^3$H]E217βG (49 Ci/mmol), [$^3$H]TCA (3.5 Ci/mmol) and [$^{14}$C]urea (40 mCi/mmol) were purchased from Perkin Elmer Life Sciences (Boston, MA, USA). All cell culture media and reagents were obtained from Invitrogen (Carlsbad, CA, USA), except FBS (Cansera, Ontario, Canada). All other chemicals and reagents were of analytical grade and readily available from commercial sources.

Male Sprague–Dawley rats weighing 220–240 g were purchased from SLC (Shizuoka, Japan) and used in all the experiments, which were carried out according to the guidelines provided by the Institutional Animal Care Committee (Graduate School of Pharmaceutical Sciences, the University of Tokyo).

[1] Department of Biopharmaceutics, Graduate School of Pharmaceutical Sciences, The University of Tokyo, 7-3-1 Hongo, Bunkyo-ku, Tokyo 113-0033, Japan.
[2] Drug Metabolism & Physicochemical Property Research Laboratory, Daiichi Pharmaceutical, Tokyo, Japan.
[3] Division of Clinical Pharmacology and Toxicology, Department of Medicine, University Hospital Zurich, Ramistrasse 100, CH-8091 Zurich, Switzerland.
[4] Division of Nephrology, Endocrinology, and Vascular Medicine, Department of Medicine, Tohoku University Graduate School of Medicine, Sendai 980-8574, Japan.
[5] To whom correspondence should be addressed. (e-mail: sugiyama@mol.f.u-tokyo.ac.jp)

**ABBREVIATIONS:** CSF, cerebrospinal fluid; E217βG, estradiol 17β glucuronide; FBS, fetal bovine serum; HEPES, 2-[4-(2-Hydroxyethyl)-1-piperazinyl]ethanesulfonic acid; Tris, 2-Amino-2-hydroxymethyl-1,3-propanediol; OAT, organic anion transporter; OATP, organic anion transporting polypeptide; PCR, polymerase chain reaction.

0724-8741/03/0500-0720/0 © 2003 Plenum Publishing Corporation

### rOatp3 mRNA Tissue Expression

RT-PCR analysis was used to compare the expression of rOatp1, rOatp2, and rOatp3 mRNA in the CP. The CP was isolated from the lateral ventricles, and total cellular RNA was prepared using a High Pure RNA Isolation kit (Roche Diagnostics GmbH, IN) according to the manufacturer's protocol. Total cellular RNA from Sprague–Dawley rat liver was prepared by a single-step guanidinium thiocyanate procedure. The RNA was then reverse transcribed using a random-hexamer primer (Takara, Japan). Primers were designed based on the nucleotide sequence of NM_017111 (rOatp1), U95011 (rOatp2), and AF041105 (rOatp3) from the region with the highest homology among rOatp1~3. The sense primer was 5′-TGGCGCTTTGATAGACAGAA-3′, and the antisense primer was 5′-CAGCTTCGTTTTCAGTTCTC-3′. Using this set of primers, PCR was performed using cDNA from the CP. The protocol for PCR was as follows: 94°C for 30 s, 55°C for 30 s and 72°C for 30 s, 30 cycles, and 68°C for 5 min. These primers enclosed the region containing the nucleotide sequences 1787–2096 of rOatp1, 1815–2115 of rOatp2 and 1701–2010 of rOatp3, respectively. The identity of the RT-PCR products was established by restriction analysis using three enzymes (*Hind*III, *Pst*I and *Bst*XI). The PCR products from rOatp2 and rOatp3 include the *Bst*XI site, whereas the restriction sites for *Hind*III and *Pst*I are specific for rOatp2 and rOatp3, respectively. They were also isolated using pGEM-T Easy Vector Systems (Promega, WI, USA), and the nucleotide sequence was confirmed by the dye-termination method.

### Real-Time PCR

Real-time PCR was performed using ABI PRISM 7700 Sequence Detection System (Applied Biosystems, Tokyo, Japan). First, RNA from the CP and liver was reverse transcribed. The cDNA in each sample were made into fixed quantity of GAPDH and amplified using TaqMan Universal PCR Master Mix Regents, 0.9 μM of primer of the respective genes, and 0.1 μM TaqMan MGB probe in a total volume of 25 μl. Each sample was analyzed in duplicate. For rOatp1, the sense primer was 5′ CCCATATGCCTCGGGTATCTAAT 3′, the antisense primer was 5′ TGCTGCATTGTCACAGGTCAA 3′, and the TaqMan MGB probe was 5′ CTGCATACCTAGCATTTTGCCTATCGGTGT 3′. For rOatp3, the sense primer was 5′ GATGTGGATGGAACTAACAATGACA 3′, the antisense primer was 5′ CACACTTGTAAGGATGAGAAGCATGT 3′, and the TaqMan MGB probe was 5′ TCATGAAGAGCCTCTCCTGCAATCCGAT 3′. The PCR mixture was pre-incubated at 50°C for 2 min followed by incubation at 95°C for 10 min and amplified by 40 cycles at 95°C for 15 s and 60°C for 1 min. The amount of mRNA was determined from a standard curve constructed of serial dilutions of a known quantity of cDNA that was the PCR amplification domain of rOatp1 or rOatp3. Standard samples were run in parallel during each analysis. The coefficient of correlation between threshold cycle and starting amount was $r > 0.996$. The amount of rOatp1 and rOatp3 in each sample was normalized by the GAPDH content.

### Antiserum and Western Blot Analysis

Antiserum against rOatp3 was raised in rabbits against a synthetic peptide consisting of the 13 carboxyl-terminal amino acids of rOatp3. Membrane fractions were prepared from LLC-PK1 cells expressing rOatp1 and rOatp3 as described previously (24). The membrane fractions and CP isolated from the lateral ventricles were diluted with loading buffer (BioLabs, Hertfordshire, UK). These specimens were boiled for 3 min then loaded onto a 10% SDS-polyacrylamide electrophoresis gel with a 4.4% stacking gel. For Western blotting, the proteins were electrophoretically transferred to a polyvinylidene difluoride (PVDF) membrane (Amersham Pharmacia Biotech, UK) using a blotter (Trans-blot; Bio-Rad, Richmond, CA, USA) at 15 V for 1 h. The membrane was blocked with Tris-buffered saline containing 0.05% Tween 20 (TBS-T) and 5% skimmed milk for 1h at room temperature. After washing with TBS-T, the membrane was incubated with anti-rOatp3 serum (dilution 1:1000). The membrane was then allowed to bind a horseradish peroxidase-labeled anti-rabbit IgG antibody (Amersham Pharmacia Biotech, UK) diluted 1:5000 in TBS-T for 1 h at room temperature followed by washing with TBS-T.

### Immunohistochemical Study

Frozen sections from male Sprague–Dawley rats for immunohistochemical study were prepared after fixing in acetone at 4°C for 10 min. Endogenous peroxidase was inactivated by incubation with Peroxidase Blocking Reagent (DAKO, Carpinteria, CA, USA) for 10 min at room temperature. After washing the sections three times with TBS-T, nonspecific protein binding was blocked by incubation with Non-Specific Staining Blocking Reagent (DAKO). Sections were incubated with anti-rOat3 antibodies (1:200) for 1 h at room temperature, washed three times with TBS-T, and subsequently incubated with the HRP-labeled secondary antibodies for 1 h at room temperature. The immune reaction was visualized using diaminobenzidine and then nuclei were stained with Methyl Green.

### Uptake of E217βG and TCA by Rat Isolated CP

Male Sprague–Dawley rats weighing 250–300 g were purchased from SLC (Shizuoka, Japan). The uptake of [$^3$H]E217βG and [$^3$H]TCA by isolated rat CP was examined by centrifugal filtration as described in detail previously (25). The CP was isolated from the lateral ventricles and incubated at 37°C for 1 min in 500 μl artificial CSF, consisting of 122 mM NaCl, 25 mM $NaHCO_3$, 10 mM glucose, 3 mM KCl, 1.4 mM $CaCl_2$, 1.2 mM $MgSO_4$, 0.4 mM $K_2HPO_4$, and 10 mM HEPES (pH 7.3), equilibrated with 95% $O_2$/5% $CO_2$. Radiolabeled ligands, with or without inhibitors, were added to initiate uptake. The tissue-to-medium concentration ratio of [$^3$H]E217βG and [$^3$H]TCA was calculated with [$^{14}$C]urea as a cell water space marker and corrected for adherent water space as described previously (25). The $^3$H and $^{14}$C activities of the specimens were determined in a liquid scintillation spectrophotometer (LS6000SE; Beckman Coulter, Fullerton, CA, USA).

### Uptake Studies in cDNA Transfected LLC-PK1 Cells

LLC-PK1 cells expressing rOatp1 were established previously (24) and LLC-PK1 cells expressing rOatp3 were established in this study. The cDNA encoding rOatp3 was inserted into the pcDNA3.1(+) mammalian expression vector

(Invitrogen, CA). Transfection of this construct was carried out using lipofectamine according to the manufacturer's protocol. The cells were maintained in a selection medium containing G418 (600 μg/ml) to select gene-transfected cells. Among the G418-resistant clones, the stable transfectants expressing rOatp3 were selected by Northern blot analysis. The rOatp3 expressing clone, which exhibited the highest transport activity for E217βG, was maintained in the presence of G418 (400 μg/ml) and used in all subsequent experiments.

Cells were seeded on a 12-well dish (Becton Dickinson, Franklin Lakes, NJ) at a density of $1.2 \times 10^5$ cells/well and cultured for 3 days. Sodium-butyrate (5 mM) was added to the culture medium to induce expression of the transporter 24 h before starting the experiments (Sugiyama *et al.* 2001). Uptake was initiated by adding medium containing radiolabeled ligands after cells had been washed twice and preincubated with Krebs–Henseleit buffer at 37°C for 15 min. This buffer consists of 142 mM NaCl, 23.8 mM $Na_2CO_3$, 4.83 mM KCl, 0.96 mM $KH_2PO_4$, 1.20 mM $MgSO_4$, 12.5 mM HEPES, 5 mM glucose, and 1.53 mM $CaCl_2$ adjusted to pH 7.4. The uptake was terminated at a designed time by adding ice-cold Krebs–Henseleit buffer. The medium was rapidly aspirated and cells were rinsed twice with ice-cold buffer. Cells were kept overnight in 500 μl 1 N NaOH for lysis. The radioactivity associated with the cells and medium was determined by liquid scintillation counting after adding 2 mL scintillation fluid (Hionic-Fluor, Packard, Meriden, CT, USA) to the vials. Protein concentration was determined by the method of Lowry with bovine serum albumin as a standard.

### Kinetic Analyses

Kinetic parameters were obtained using the following equation (Michaelis–Menten equation) except for Oatp1-mediated uptake:

$$v = V_{max} \cdot S/(K_m + S)$$

where $v$ is the uptake rate of the substrate (pmol/min/mg protein or pmol/min/μl tissue), S is the substrate concentration in the medium (μM), $K_m$ is the Michaelis–Menten constant (μM) and $V_{max}$ is the maximum uptake rate (pmol/min/mg protein or pmol/min/μl tissue).

In the case of Oatp1-mediated uptake of E217βG, Eadie–Hofstee plot (see Fig. 3 later) suggested the presence of non-saturable component. To obtain the kinetic parameters, the following equation was used for fitting;

$$v = V_{max} \cdot S/(K_m + S) + P_{dif} \cdot S$$

where $P_{dif}$ represents the uptake clearance corresponding to the non-saturable component (μl/min/mg protein or μl/min/μl tissue). To obtain the kinetic parameters, the equation was fitted to the uptake velocity using a MULTI program (26). The input data were weighted as the reciprocals of the observed values and the Damping Gauss Newton Method algorithm was used for fitting. Inhibition constants ($K_i$) of several compounds were calculated assuming competitive inhibition.

## RESULTS

### Expression of rOatp1 and rOatp3 mRNA in the CP

The expression of rOatp1 and rOatp3 in the CP was examined by RT-PCR (Fig. 1). The size of the PCR product

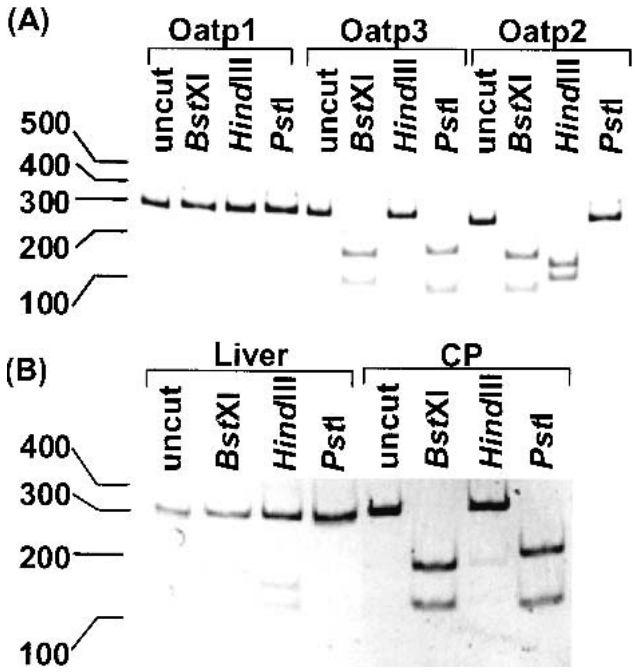


**Fig. 1.** Expression of rOatp1 and rOatp3 in the liver and CP. RT-PCR and restriction analysis was carried out to identify rOatp3 mRNA in rat CP. Reverse transcription and PCR was performed as described in Methods. The restriction pattern of the PCR products obtained using rOatp1~3 cDNA as a template is shown in panel A, and the restriction patterns of the PCR products from the liver and CP cDNA are shown in panel B.

from the liver and CP was approximately 300 bp, as expected from the positions of the primers in the nucleotide sequences of rOatp1~3 (Figs. 1A, 1B). To further establish the identity of the product, restriction analysis of these products was performed with three different enzymes (*Hin*dIII, *Pst*I, and *Bst*XI). As expected from the known restriction map of rOatp1~3 cDNA, the restriction site by *Bst*XI is included in the PCR products from rOatp2 and rOapt3 but the sites by *Hind* III and *Pst* I are included in rOatp2 and rOatp3, respectively (Fig. 1A). Following treatment by these three restriction enzymes, the isoform expressed in the CP can be identified. The restriction pattern of the PCR products prepared using CP cDNA with all three enzymes was different from that prepared using liver cDNA (Fig. 1B). The restriction pattern of the PCR products from the liver was exactly as expected from the known restriction map of rOatp1 cDNA, and a faint pattern corresponding to rOatp2 was observed (Fig. 1b). In contrast, the restriction pattern of the PCR products from the CP was exactly as expected from the known restriction map of rOatp3 cDNA, but not rOatp1 or rOatp2 cDNA (Fig. 1b). This was confirmed by real-time PCR using a TaqMan MGB probe. The amounts of rOatp1 and rOatp3 mRNA was corrected by GAPDH in the CP and found to be 0.087 (0.085 and 0.088) and 28 (29 and 26), respectively, whereas the amounts of rOatp1 and rOatp3 mRNA in the liver was 42 (46 and 38) and 0.0064 (0.0075 and 0.0053), respectively.

### Expression and Localization of rOatp3 on Rat CP

Using the antiserum against rOatp3, immunoreactive protein was detected at approximately 80 kDa in LLC-PK1

cells expressing rOatp3, and no band was observed in vector-transfected LLC-PK1 cells (Fig. 2a). A faint band was also detected at the same molecular weight in LLC-PK1 cells expressing rOatp1 (Fig. 2a, lane 2). The band was also detected in the CP at the same size as detected in LLC-PK1 cells expressing rOatp3 (Fig. 2a).

Immunohisotchemical staining was performed using the antiserum against rOatp3 to determine the localization of rOatp3 in the CP. The basal surface of the choroid epithelial cells is apposed to a capillary bed, whereas the brush border surface, covered with microvilli, faces the CSF. The positive signals detected by the antiserum were localized along the surface facing the CSF, but not the surface facing the capillary bed (Fig. 2b), suggesting that rOatp3 is localized along the brush border membrane of the choroid epithelial cells.

### Uptake of E217βG by LLC-PK1 Cells Expressing rOatp1 and rOatp3

The time-profiles of the uptake of E217βG by rOatp1 and rOatp3 are shown in Fig. 3. The uptake of E217βG by LLC-PK1 cells expressing rOatp1 and rOatp3 was significantly greater than that by vector-transfected cells (Figs. 3A, C). Because the uptake of E217βG by rOatp1 and rOatp3 increased linearly up to 5 min of incubation (Figs. 3A, C), the uptake of E217βG at 5 min was used for further studies. The uptake of E217βG by rOatp1 and rOatp3 was saturated at higher substrate concentrations (Fig. 3B, D). The $K_m$ and $V_{max}$ values for the uptake of E217βG by rOatp1 and rOatp3 were determined to be 2.33 ± 0.63 μM, 4.52 ± 0.99 pmol/min/mg protein, and 1.15 ± 0.26 μM and 3.72 ± 0.26 pmol/min/mg protein, respectively. The uptake clearance corresponding to the non-saturable component of the uptake of E217βG by rOatp1 was 0.193 ± 0.032 μl/min/mg protein., and this may be ascribed to the experimental deviation between the uptake in vector-transfected and Oatp1-expressed cells.

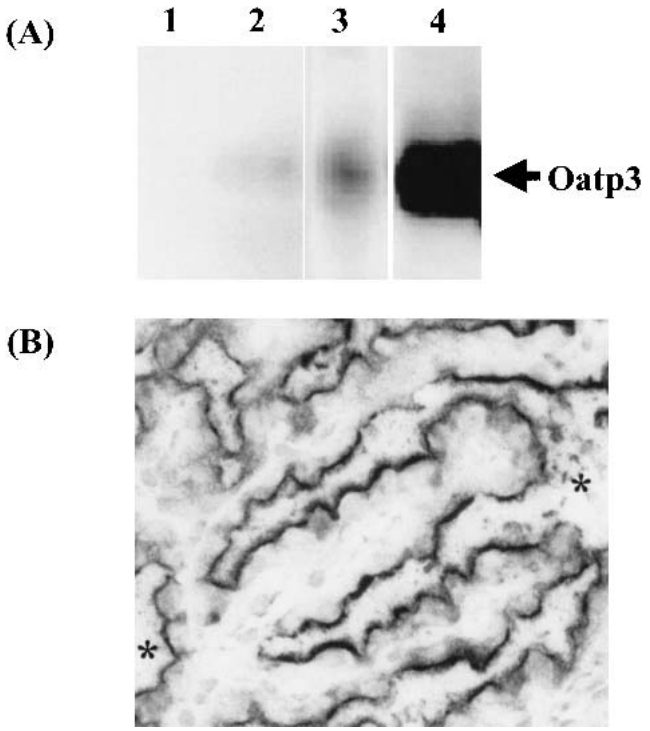


**Fig. 2.** Localization of rOatp3 in the rat CP. (A) Crude membrane fractions from vector-transfected LLC-PK1 cells, and LLC-PK1 cells expressing rOatp1 and rOatp3 (lanes 1~3; 3 μg/lane) and rat CP (lane 4; 3.3 μg/lane) were separated by SDS-PAGE (10% separating gel) as described in Materials and Methods. rOatp3 was detected by the antiserum against a region near the carboxyl terminus of rOatp3. (B) Cryosections of brain from male Sprague–Dawley rats were incubated with rOatp3-antiserum. The immune reaction was visualized using diaminobenzidine, and then nuclei were stained with Methyl Green (×200). The positive signals detected by the antiserum against rOatp3 were along the surface facing the CSF. Asterisk indicates the CSF space.

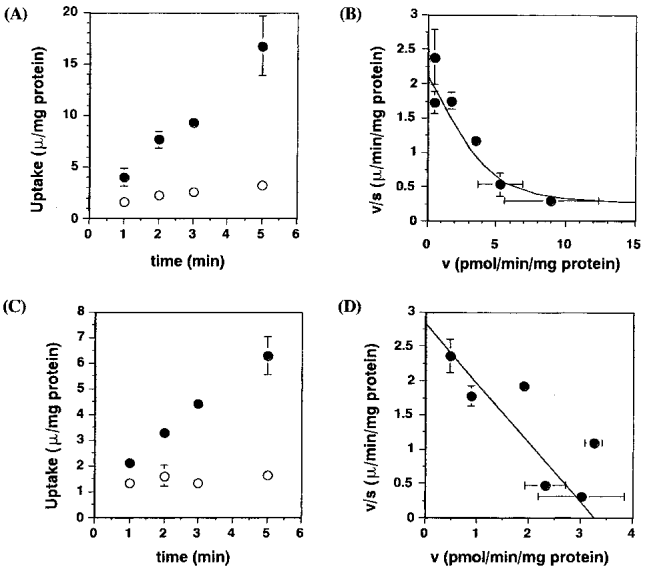


**Fig. 3.** Uptake of [$^3$H]E217βG by LLC-PK1 cells expressing rOatp1 and rOatp3 and the concentration dependence of their uptake. The uptake of [$^3$H]E217βG by rOatp1 (A) and rOatp3 (C) was examined at 37°C. Closed circles represent the uptake by LLC-PK1 cells expressing rOatp1 in panel (A) and rOatp3 in panel (C), whereas open circles represent the uptake by vector-transfected cells. Uptake was initiated by adding the uptake buffer containing [$^3$H]E217βG (0.2 μM) and terminated at designated times by adding ice-cold buffer. The concentration-dependence of rOatp1-mediated [$^3$H]E217βG uptake (B) and rOatp3-mediated [$^3$H]E217βG uptake (D) is shown. Kinetic analyses revealed that the uptake of [$^3$H]E217βG by rOatp1 and rOatp3 consists of one saturable and one non-saturable component, and a single saturable component, respectively. Michaelis–Menten constants were obtained by non-linear regression analysis and the solid line represents the fitted line. Each point represents the mean ± SE (n = 3).

The effect of inhibitors on rOatp1- and rOatp3-mediated E217βG uptake was examined (Fig. 4). Assuming competitive inhibition, the $K_i$ values of inhibitors for rOatp1 and rOatp3 were determined as summarized in Table I. Glibenclamide and estrone-3-sulfate are potent inhibitors of rOatp1 and rOatp3, and corticosterone diclofenac, indomethacin, and taurocholate are moderate inhibitors whereas probenecid and quinine are weak inhibitors of rOatp1 and rOatp3. The $K_i$ values of rOatp1 and rOatp3 were quite similar (Table I). Digoxin (an inhibitor of rOatp2), PAH and cimetidine (inhibitors of rOat3) did not affect the uptake by rOatp1 and rOatp3 (data not shown).

### Uptake of E217βG and TCA by Isolated Rat CP

The time-profiles of the uptake of E217βG and TCA by isolated rat CP are shown in Figs. 5A, 5C. The uptake of

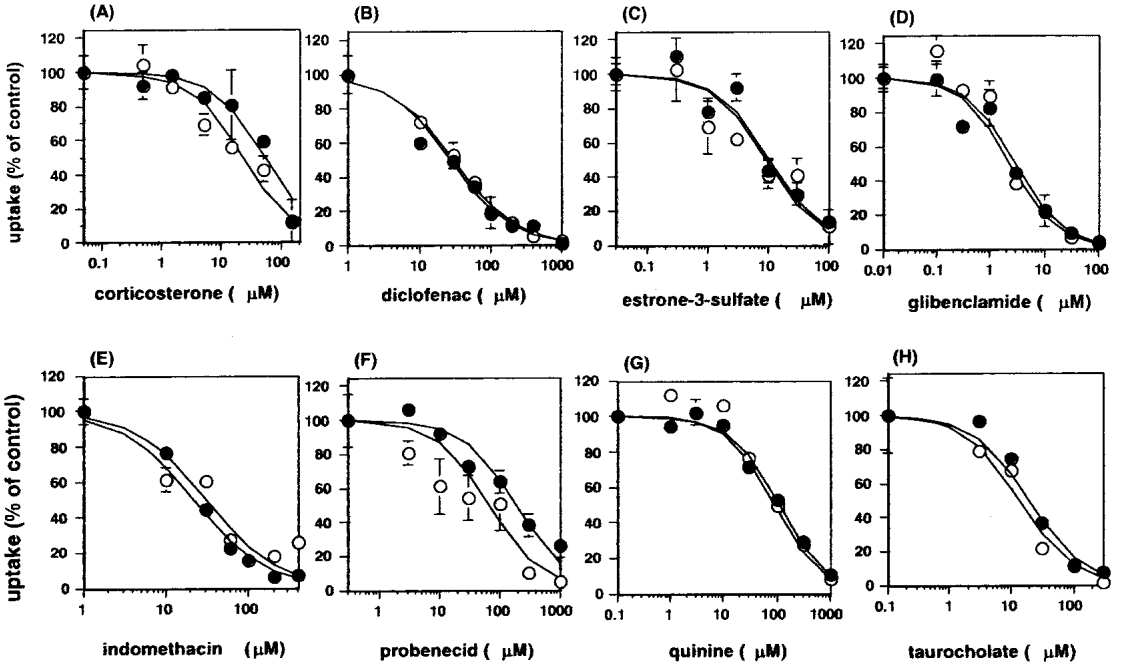


**Fig. 4.** Inhibitory effect on the uptake of E217βG by rOatp1 and rOatp3. The uptake of [$^3$H]E217βG (0.2 μM) by rOatp1 and rOatp3 was determined in the presence and absence of inhibitors ((A) corticonterone, (B) diclofenac, (C) estrone-3-sulfate, (D) glibenclamide, (E) indomethacin (F) probenecid, (G) quinine, (H) taurocholate) at the concentrations indicated. Closed and open symbols represent the rOatp1- and rOatp3-mediated uptake of [$^3$H]E217βG. The inhibition constants ($K_i$) were calculated assuming competitive inhibition. The solid lines represent the fitted line obtained by non-linear regression analysis. The details of fitting are described in Materials and Methods. Each point represents the mean ± SE (n = 3).

E217βG and TCA by isolated rat CP increased linearly up to 5 min of incubation. Their uptake at 3 min was used to examine the concentration-dependence and the effect of various inhibitors. The Eadie–Hofstee plot indicates that the uptake of E217βG and TCA by rat isolated CP consists of one saturable component (Figs. 5B, 5D). The $K_m$ and $V_{max}$ values for the uptake of E217βG and TCA by isolated rat CP were determined to be 55.5 ± 8.1 μM and 554 ± 69 pmol/min/μl tissue, and 116 ± 17 μM and 1010 ± 109 pmol/min/μl tissue, respectively. The uptake of E217βG by isolated rat CP under linear conditions ($V_{max}/K_m$) was comparable with that of TCA.

**Table I.** Inhibition Constants (Ki values) for the Uptake of E217βG by Isolated Rat CP, rOatp1 and rOatp3

| | Choroid plexus $K_i$ (μM) | Oatp1 $K_i$ (μM) | Oatp3 $K_i$ (μM) |
|---|---|---|---|
| corticosterone | 47.4 ± 9.6 | 23.0 ± 6.4 | 53.8 ± 14.4 |
| diclofenac | 236 ± 49 | 30.6 ± 2.5 | 27.3 ± 4.8 |
| estrone sulfate | 77.5 ± 20.8 | 9.37 ± 4.27 | 10.4 ± 3.7 |
| glibenclamide | N.D.[a] | 2.37 ± 0.63 | 2.96 ± 0.81 |
| ibuprofen | 760 ± 226 | N.D.[a] | N.D.[a] |
| indomethacin | 30.9 ± 7.4 | 30.8 ± 12.3 | 21.8 ± 2.6 |
| probenecid | 635 ± 320 | 66.2 ± 29.7 | 187 ± 50 |
| quinine | 260 ± 58 | 89.1 ± 14.9 | 109 ± 15 |
| taurocholate | 124 ± 8 | 13.3 ± 3.1 | 19.0 ± 3.8 |

*Note:* Data shown in the Figure 4 and 6 were used to determine the $K_i$ values for the uptake of E217βG by isolated rat CP, rOatp1- and rOatp3 cDNA-transfected cells. Details of the uptake studies were described in Methods.

[a] N.D. Not Determined.

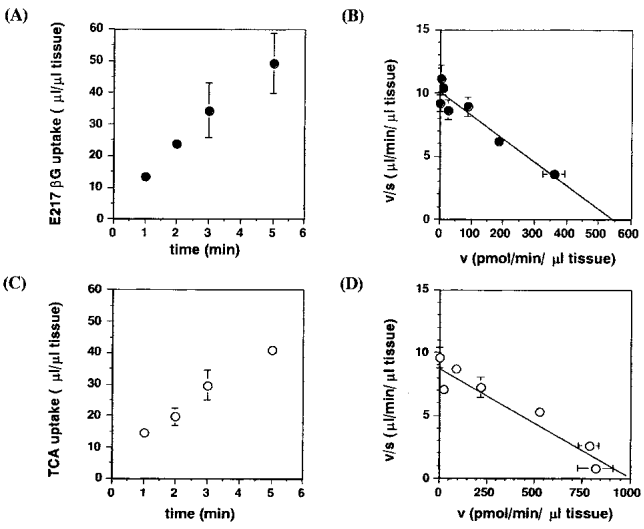


**Fig. 5.** Uptake of [$^3$H]E217βG and [$^3$H]TCA by isolated rat CP and concentration dependence of their uptake by isolated rat CP. The CP was isolated from the lateral ventricles. The uptake of [$^3$H]E217βG (0.01 μM) (A) and [$^3$H]TCA (0.15 μM) (B) by isolated rat CP was examined by centrifugal filtration as described in Materials and Methods. The tissue-to-medium concentration ratio of [$^3$H]E217βG and [$^3$H]TCA was calculated with [$^{14}$C]urea as a cell water space marker and was corrected for the adherent water space. Closed and open circles represent the uptake of [$^3$H]E217βG and [$^3$H]TCA by isolated CP, respectively (A, C). The concentration-dependence of the uptake of [$^3$H]E217βG (B) and [$^3$H]TCA (D) by isolated rat CP is shown as an Eadie–Hofstee plot. The uptake determined at 3 min with different substrate concentrations of E217βG and TCA was used for the calculation. The solid line represents the fitted line. Each point represents the mean ± SE (n = 3).

### Effect of Inhibitors on the Uptake of E217βG by Isolated Rat CP

To evaluate the contribution of organic anion transporters to the uptake of E217βG by isolated rat CP, inhibition studies were carried out (Fig. 6). Digoxin is a specific inhibitor of rOatp2 (24), whereas benzylpenicillin, PAH and cimetidine are specific for rOat3 (11). Corticosterone, estrone-3-sulfate and indomethacin are moderate inhibitors of the uptake of E217βG by the CP with $K_i$ values of 47.4 ± 9.6, 77.5 ± 20.8, and 30.9 ± 7.4 μM, respectively, and diclofenac, ibuprofen, probenecid, quinine, and taurocholate are weak inhibitors with $K_i$ values of 236 ± 49, 760 ± 226, 635 ± 320, 260 ± 58, and 124 ± 8 μM, respectively (Table I). The effect of digoxin, benzylpenicillin, PAH, and cimetidine was low or zero for the uptake of E217βG by isolated rat CP (data not shown).

## DISCUSSION

In this article, we have demonstrated the expression and localization of rOatp3 on isolated rat CP[1], the involvement of rOatp3 in the uptake of E217βG and, possibly, TCA by isolated rat CP was investigated using rat isolated CP.

The expression of rOatp3 in the CP was studied by RT-PCR and Western blot analyses. The restriction pattern of PCR products from rat CP cDNA was consistent with that of rOatp3, but not rOatp1, suggesting that the major transporter expressed in the CP is rOatp3. This was confirmed by real-time PCR and a TaqMan MGB probe designed for rOatp1 and rOatp3. The mRNA expression of rOatp3 is more abundant than that of rOatp1in the CP, whereas the mRNA expression of rOatp3 in the liver is low. The latter finding is consistent with previous reports (22,23). The expression of rOatp3 protein in rat CP was examined by Western blot analysis. Although a single band was detected in the CP and LLC-PK1 cells expressing rOatp3, which was not detected in the vector-transfected LLC-PK1 cells, using the antiserum against rOatp3, a faint band was also detected in LLC-PK1 cells expressing rOatp1 (Fig. 2). It is likely that the antiserum against rOatp3 prepared in this study cross-reacts with rOatp1. These results were contradictory to the previous report in which the expression of rOatp1 was detected in the CP by RT-PCR *in situ* hybridization and Western blot analyses (12). The nucleotide and amino acid sequences of rOatp3 exhibit high homology to rOatp1 (80 and 86%, respectively). Therefore, it is likely that the probes for rOatp1 reacted with rOatp3 mRNA or protein in the CP in the previous report (12). Immunohistochemical staining detected positive signals along the brush border membrane of the choroid epithelial cells. Taking the abundant expression of rOatp3 mRNA in the CP into consideration, the positive signal along the apical membrane of the choroid epithelial cells must be ascribed to rOatp3. A monoclonal antibody, specifically reacting with each Oatp isoform (rOatp1~3), needs to be established for further analyses.

To investigate the contribution of rOatp3 to the total uptake of rOatp3 substrates, inhibitors selective for rOatp3 are necessary. The selectivity of inhibitors for rOatp1 and rOatp3 was investigated using cDNA-transfected cells. Transfection of rOatp3 cDNA to LLC-PK1 cells resulted in a significant increase in the intracellular accumulation of E217βG. The uptake was saturable with a $K_m$ value of 1.2 μM that is comparable with that for rOatp1 (Table I). Glibenclamide and estrone-3-sulfate are potent inhibitors of rOatp3, corticosterone, diclofenac, indomethacin, and taurocholate are moderate inhibitors, whereas probenecid and quinine are weak inhibitors of rOatp3. Comparison of the $K_i$ values for

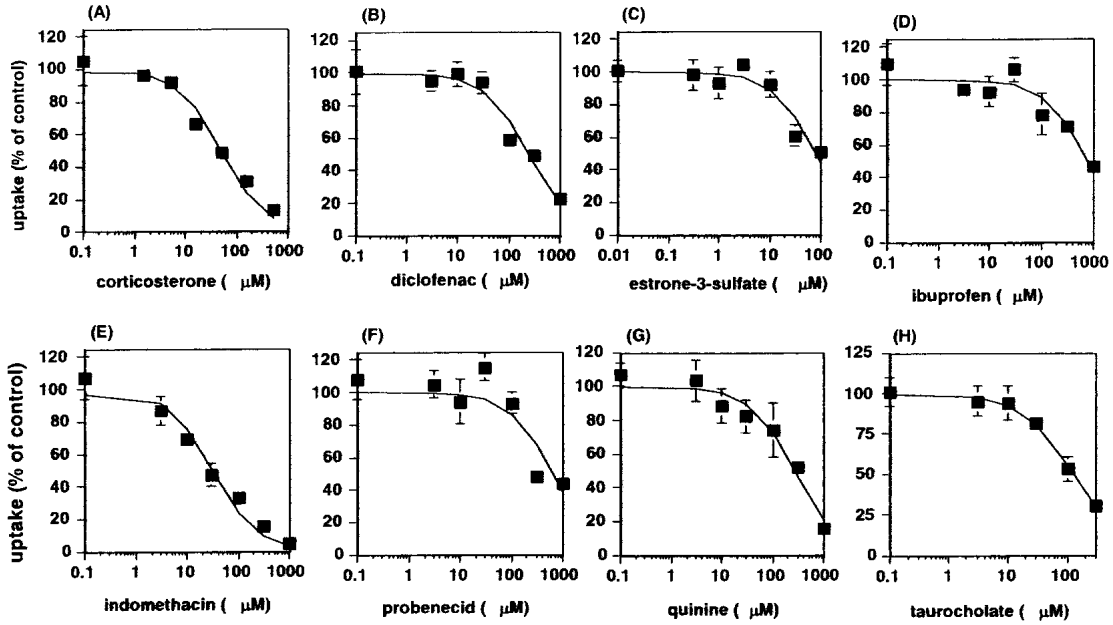


**Fig. 6.** Inhibitory effect on the uptake of [$^3$H]E217βG by isolated rat CP. The uptake of [$^3$H]E217βG (0.01 μM) by isolated rat CP was determined at 3 min in the presence and absence of inhibitors ((A) corticonterone, (B) diclofenac, (C) estrone-3-sulfate, (D) ibuprofen, (E) indomethacin (F) probenecid, (G) quinine, (H) taurocholate) at the concentrations indicated. The inhibition constants ($K_i$) were calculated assuming competitive inhibition. The solid lines represent the fitted line obtained by non-linear regression analysis. The details of fitting are described in Materials and Methods. Each point represents the mean ± SE (n = 3).

rOatp1 and rOatp3 indicates that the substrate specificity of rOatp1 and rOatp3 is similar. Although digoxin is a substrate of rOatp3 (20), no inhibitory effect on rOatp3 was observed, suggesting that the affinity of digoxin for rOatp3 is low, as reported previously (20). Digoxin can be used as inhibitor that distinguishes rOatp2-mediated transport from rOatp1- and rOatp3-mediated transport. However, no selective inhibitor for rOatp1 or rOatp3 was found in this study.

The previous report on $K_m$ value of E217βG for rOatp3 was 39 μM, 30-fold lower than the $K_m$ value in this study, in an experiment using rOatp3-cRNA injected oocytes, whereas the $K_i$ value of estrone-3-sulfate determined in this study was 27-fold higher than that in rOatp3-cRNA injected oocytes (20). The $K_i$ and $K_m$ values of E217βG and TCA were comparable in these two different expression systems (20,21). The reason for these discrepancies remains unknown, and further studies are required.

Using isolated rat CP, the transport properties across the brush-border membrane were characterized. Significant accumulation of E217βG was observed in isolated rat CP as reported previously (9). The absolute value of the uptake of E217βG by isolated rat CP at 3 min was 2-fold greater than the previous reported values, however, a marked difference was observed in the fraction of saturable component to the total uptake. Although 40% of the accumulation was associated with the saturable component in a previous report, the Eadie–Hofstee plot indicates that the uptake was predominantly accounted for by a saturable component alone in this study. The intrinsic transport activity of E217βG by isolated rat CP ($V_{max}/K_m$) was almost 10-fold greater than previous reported values (9). The intrinsic transport activity of TCA by isolated rat CP was comparable with that of E217βG. The $K_m$ value for the uptake of TCA by rat isolated CP was determined to be 119 μM, and the value was comparable with the $K_i$ value of TCA for the uptake of E217βG by the CP (124 μM), suggesting that TCA shares the same uptake mechanism with E217βG on the brush border membrane.

The $K_m$ value determined in this study (55 μM) was 16-fold greater than in the previous report (3.4 μM). In addition, the $K_m$ values of E217βG and TCA for their uptake by isolated rat CP were 45- and 6-fold greater than those for rOatp3 (Table I). The Ki values of diclofenac and estrone-3-sulfate for the uptake of E217βG by isolated rat CP were 7- and 10-fold greater than those for rOatp3 whereas the difference in the $K_i$ values of corticosterone, probenecid, and quinine was less than 3-fold (Table I). Although the kinetic parameters of some compounds exhibited difference between rOatp3-expressed LLC-PK1 cells and the CP, taking the localization and substrate specificity of rOatp3 into consideration, it is likely that rOatp3 is involved in the uptake of amphipathic organic anions by the CP. To support this, further studies are required by examining the uptake of rOatp3-specific substrates by the CP and the effect of rOatp3-selective inhibitors. The reason for the difference in kinetic parameters is unknown. It is possible that the affinity of ligands for rOatp3 differs depending on the expression system. Because digoxin, PAH, PCG, and benzylpenicillin did not affect the uptake of E217βG by isolated rat CP, the involvement of rOat3 and rOatp2 can be excluded. rOatp2 has been shown to be localized on the basolateral membrane of the choroid epithelial cells (1). Taking the localization of rOatp2 in the CP into consideration, it is rational that digoxin did not affect the uptake of E217βG by the CP at all because the uptake determined using isolated rat CP occurs mainly through the brush border membrane.

In conclusion, our studies suggest that rOatp3 is involved in the uptake of E217βG by the CP, and acts as one of the detoxification systems that removes xenobiotics and drugs from the CSF.

## ACKNOWLEDGMENT

This work was supported by Grants-in-Aid from the Ministry of Health, Labor and Welfare of Japan.

## REFERENCES

1. B. Gao and P. J. Meier. organic anion transport across the choroid plexus. *Microsc. Res. Tech.* **52**:60–64 (2001).
2. R. Spector. Drug transport in the mammalian central nervous system: multiple complex systems. *Pharmacol.* **60**:58–73 (2000).
3. J. F. Ghersi–Egea and N. Strazielle. Brain drug delivery, drug metabolism, and multidrug resistance at the choroid plexus. *Microsc. Res. Tech.* **52**:83–88 (2001).
4. H. Kusuhara and Y. Sugiyama. Efflux transport systems for drugs at the blood-brain barrier and blood- cerebrospinal fluid barrier (Part 2). *Drug Discov. Today* **6**:206–212 (2001).
5. H. Kusuhara and Y. Sugiyama. Efflux transport systems for drugs at the blood-brain barrier and blood- cerebrospinal fluid barrier (Part 1). *Drug Discov. Today* **6**:150–156 (2001).
6. H. Kusuhara and Y. Sugiyama. Role of transporters in the tissue-selective distribution and elimination of drugs: transporters in the liver, small intestine, brain and kidney. *J. Control. Release* **78**:43–54 (2002).
7. M. Haselbach, J. Wegener, S. Decker, C. Engelbertz, and H. J. Galla. Porcine Choroid plexus epithelial cells in culture: regulation of barrier properties and transport processes. *Microsc. Res. Tech.* **52**:137–152 (2001).
8. N. Strazielle and J. F. Ghersi–Egea. Demonstration of a coupled metabolism-efflux process at the choroid plexus as a mechanism of brain protection toward xenobiotics. *J. Neurosci.* **19**:6275–6289 (1999).
9. J. Nishino, H. Suzuki, D. Sugiyama, T. Kitazawa, K. Ito, M. Hanano, and Y. Sugiyama. Transepithelial transport of organic anions across the choroid plexus: possible involvement of organic anion transporter and multidrug resistance-associated protein. *J. Pharmacol. Exp. Ther.* **290**:289–294 (1999).
10. T. Kitazawa, K. Hosoya, T. Takahashi, Y. Sugiyama, and T. Terasaki. In-vivo and in-vitro evidence of a carrier-mediated efflux transport system for oestrone-3-sulphate across the blood-cerebrospinal fluid barrier. *J. Pharm. Pharmacol.* **52**:281–288 (2000).
11. Y. Nagata, H. Kusuhara, H. Endou, and Y. Sugiyama. Expression and functional characterization of rat organic anion transporter 3 (rOat3) in the choroid plexus. *Mol. Pharmacol.* **61**:982–988 (2002).
12. R. H. Angeletti, P. M. Novikoff, S. R. Juvvadi, J. M. Fritschy, P. J. Meier, and A. W. Wolkoff. The choroid plexus epithelium is the site of the organic anion transport protein in the brain. *Proc. Natl. Acad. Sci. USA* **94**:283–286 (1997).
13. H. Suzuki, T. Terasaki, and Y. Sugiyama. Role of efflux transport across the blood-brain barrier and blood-cerebrospinal fluid barrier on the disposition of xenobiotics in the central nervous system. *Adv. Drug Deliv. Rev.* **25**:257–285 (1997).
14. H. Ishizuka, K. Konno, H. Naganuma, K. Nishimura, H. Kouzuki, H. Suzuki, B. Stieger, P. J. Meier, and Y. Sugiyama. Transport of

[1] Dr. Terasaki and his collaborator (Tohoku University, Miyagi, Japan) also demonstrated the expression and localization of rOatp3 on the brush border membrane of the choroid epithelial cells by RT-PCR using primers specifically designed for rOatp1, rOatp2 and rOatp3 and immunohistochemical studies in the annual meeting of Japanese Society for the Study of Xenobiotics (Takizawa *et al.*, *Xenobio. Metabol. Dispos.* **16**:S277).

temocaprilat into rat hepatocytes: role of organic anion transporting polypeptide. *J. Pharmacol. Exp. Ther.* **287**:37–42 (1998).
15. T. N. Abu–Zahra, A. W. Wolkoff, R. B. Kim, and K. S. Pang. Uptake of enalapril and expression of organic anion transporting polypeptide 1 in zonal, isolated rat hepatocytes. *Drug Metab. Dispos.* **28**:801–806 (2000).
16. P. J. Meier, U. Eckhardt, A. Schroeder, B. Hagenbuch, and B. Stieger. Substrate specificity of sinusoidal bile acid and organic anion uptake systems in rat and human liver. *Hepatology* **26**: 1667–1677 (1997).
17. M. Muller and P. L. Jansen. Molecular aspects of hepatobiliary transport. *Am. J. Physiol.* **272**:G1285–G1303 (1997).
18. C. Reichel, B. Gao, J. Van Montfoort, V. Cattori, C. Rahner, B. Hagenbuch, B. Stieger, T. Kamisako, and P. J. Meier. Localization and function of the organic anion-transporting polypeptide Oatp2 in rat liver. *Gastroenterology* **117**:688–695 (1999).
19. P. J. Meier and B. Stieger. Bile salt transporters. *Annu. Rev. Physiol.* **64**:635–661 (2002).
20. V. Cattori, J. E. van Montfoort, B. Stieger, L. Landmann, D. K. Meijer, K. H. Winterhalter, P. J. Meier, and B. Hagenbuch. Localization of organic anion transporting polypeptide 4 (Oatp4) in rat liver and comparison of its substrate specificity with Oatp1, Oatp2 and Oatp3. *Pflugers Arch.* **443**:188–195 (2001).
21. T. Abe, M. Kakyo, T. Tokui, R. Nakagomi, T. Nishio, D. Nakai, H. Nomura, M. Unno, M. Suzuki, T. Naitoh, S. Matsuno, and H. Yawo. Identification of a novel gene family encoding human liver-specific organic anion transporter LST-1. *J. Biol. Chem.* **274**: 17159–17163 (1999).
22. H. C. Walters, A. L. Craddock, H. Fusegawa, M. C. Willingham, and P. A. Dawson. Expression, transport properties, and chromosomal location of organic anion transporter subtype 3. *Am. J. Physiol.* **279**:G1188–G1200 (2000).
23. N. Li, D. P. Hartley, N. J. Cherrington, and C. D. Klaassen. Tissue expression, ontogeny, and inducibility of rat organic anion transporting polypeptide 4. *J. Pharmacol. Exp. Ther.* **301**:551–560 (2002).
24. D. Sugiyama, H. Kusuhara, Y. Shitara, T. Abe, P. J. Meier, T. Sekine, H. Endou, H. Suzuki, and Y. Sugiyama. Characterization of the efflux transport of 17beta-estradiol-D-17beta- glucuronide from the brain across the blood-brain barrier. *J. Pharmacol. Exp. Ther.* **298**:316–322 (2001).
25. H. Suzuki, Y. Sawada, Y. Sugiyama, T. Iga, and M. Hanano. Transport of cimetidine by the rat choroid plexus in vitro. *J. Pharmacol. Exp. Ther.* **239**:927–935 (1986).
26. K. Yamaoka, Y. Tanigawara, T. Nakagawa, and T. Uno. A pharmacokinetic analysis program (multi) for microcomputer. *J. Pharmacobiodyn.* **4**:879–885 (1981).